


Synthesis and Wire EDM Characteristics of Cu–Al–Mn Ternary Shape Memory Alloys Using Taguchi Method

N. Praveen¹ · U. S. Mallik¹ · A. G. Shivasiddaramaih¹ ·
R. Suresh² · C. Durga Prasad³  · L. Shivaramu²

Received: 27 April 2023 / Accepted: 26 May 2023 / Published online: 5 June 2023
© The Institution of Engineers (India) 2023

Abstract Cu–Al–Mn ternary shape memory alloys (SMAs) were synthesized and investigated for their surface roughness (Ra). Cu–Al–Mn SMAs were prepared through the ingot metallurgy method with aluminium (Al) content of 10–15 wt.% and manganese (Mn) content of 0–10wt.% and the rest is copper. After the heat treatment process, the alloy which exhibited an excellent shape memory effect was subjected to machinability studies in Wire EDM (Electrical Discharge Machining). In the context of Wire EDM, experiments were carried out using Taguchi's L9 orthogonal array (OA). Taguchi's method was used to obtain the optimum value of surface roughness. The effects of pulse duration, pulse interval, and peak current on surface roughness were studied using a technique that combined orthogonal array (OA) and analysis of variance (ANOVA). The obtained results revealed that peak current is the most significant factor affecting the Ra. From the Taguchi method, the best machining parameters combination settings are pulse duration (100 μ s), pulse interval (32 μ s), and peak current (1A) to meet the optimum value of surface roughness. The main purpose of the present investigation is to check for its machinability by identifying the machining performance, material behaviour and finally to optimise wire EDM machining

parameters for Cu–Al–Mn SMAs using Taguchi's optimization technique.

Keywords Cu–Al–Mn ternary SMAs · Wire EDM · Surface roughness · Taguchi method · Regression analysis

Introduction

SMAs are the alloy which has the capability to regain its predeformed shape when subjected to heat or stresses. They are divided into two categories: ferrous alloys and non-ferrous alloys. The main alloying elements in ferrous SMA are 'Fe', 'Mn', and 'Si'. Non-ferrous alloys are more expensive than ferrous SMAs. Although certain alloys exhibit SME, it only works in one direction; moreover, these alloys exhibit some limitations on the shape memory effect itself. As a result, other alloys for SMAs must be investigated [1, 2]. Since many years ago, Cu-based alloys have been studied and compared to Ni–Ti SMAs, these Cu-based SMAs are more affordable and less difficult to process [2, 3].

Cu–Al–Mn SMAs with higher concentrations of Mn are more ductile than those with lower concentrations of Mn. This is because the parent phase of the SMA has an L21 structure with a lesser degree of order. When the material is quenched, the disordered phase in Cu–Al–Mn SMAs changes into martensite from the state in which it is stable at high temperatures. Three different types of martensites, α_1 (3R), β_1 (18R), and γ_1 (2H), obtained in the different composition ranges of the alloys depending on the amount of aluminium and manganese present. Manganese stabilizes the BCC phase with lowering the degree of order, and enhances the ductility of a binary Cu–Al alloy [4, 5]. The transformation temperature of these alloys is very sensitive to variations in Al and Mn concentrations. These Cu–Al–Mn alloys

✉ C. Durga Prasad
durgaprasadi71@gmail.com

¹ Department of Mechanical Engineering, Siddaganga Institute of Technology, Tumkur, Karnataka 572103, India

² Department of Mechanical and Manufacturing Engineering, M.S. Ramaiah University of Applied Sciences, Bengaluru 560058, India

³ Department of Mechanical Engineering, RV Institute of Technology and Management, Bengaluru, Karnataka, India

have good strain recovery due to their two distinct characteristics. However, for some practical applications, further enhancement of the SME and PE properties of the alloys is needed. The applications of SMAs are aerospace, marine, biomedical application, etc.

In various industrial sectors, the use of non-traditional machining processes plays a major role in machining materials with high strength and complex shapes. The demand for high speed machining requires good quality surface finish with the desired tolerance. Wire EDM is also called as spark EDM. In wire EDM, there is no requirement for cutting forces to remove material from the workpiece where low residual stresses are important [6, 7]. An electrode acts as a conducting wire in the wire EDM process. During machining, thermal energy is used, and the conductive work material is eroded as a result of the electric spark. These sparks are generated between the sample and the cutting wire during the process by using dielectric fluid as an ionisation medium. The continuous flow of dielectric fluid serves as a coolant and aids in flushing away the debris that has been removed, whereas electrical sparks produce thermal energy that causes microparticles to be removed from the material.

This wire EDM processes are used in various automotive sectors, tools and die manufacturing industries, etc. The impact of input factors like T_{on} , T_{off} , voltage and current on surface roughness and optimized these process parameters by selecting the optimal combination of factors to achieve minimum value of Ra. Here, the most predominant factor for the SR is current, rest three factors has less impact as compared to current [8]. The Taguchi DOE used investigate WEDM performance characteristics like kerf width, MRR, and SR. The SR of 3.0933 m was attained as the minimal surface roughness [9]. The residual analysis as an alternative to conventional qualitative testing methods. According to the findings of an ANOVA, T_{on} and pulse peak current were the two main factors affecting on Ra of wire EDM DC-53 die steel. It was also found that increasing these two factors increased the Ra of the test specimen [10]. The Grey–Taguchi method used to optimise the wire EDM factors of the Incoloy800 super alloy with response factors like MRR, Ra, and Kerf. Gap Voltage, T_{on} , T_{off} , and Wire Feed are the process parameters examined in this study. Grey Relational Analysis (GRA) was adapted to identify the optimal factors, while ANOVA was used to find the relatively significant factor. The nonlinear regression analysis method was used to mathematically model the fluctuation of output responses with process parameters, and the models were tested for their suitability [11–14].

The impact of process parameters on CNC Wire EDM characteristics on various criteria such as specific energy consumption, surface finish, cutting speed, and spark gap was investigated in this study, and optimal values were determined. For optimal process utilisation with high productivity

is required to analyse the effects of factors in order to achieve improved machining characteristics [15–17]. The effect of EDM settings on Inconel 601 employing responsive surface methods was investigated. When the peak current is increased, the volumetric MRR increases. It was found that as wire tension is increased, the value of surface roughness also increases. This was determined to be the result of increasing the wire tension while simultaneously reducing the amount of wire bending, which created a dynamic stability condition in which the diameter and depth of the crater remained unchanged. The resulting roughness is better than before [18–21]. The cutting of $Al_2O_3p/6061Al$ composites by wire EDM using the input factors such as cutting speed, slit width, and surface roughness was varied to know how they affected machining performance characteristics. Furthermore, during machining of the $Al_2O_3p/6061Al$ composite, the wire electrode will be easily damaged [22–25].

The Taguchi method is commonly used to improve industrial and manufacturing operations. There are three steps to the Taguchi design optimization approach. Selecting the required orthogonal array (OA), conducting tests, analysing data, establishing the best condition, and running confirmation runs are all part of the Taguchi parameter design process [26–29]. The Taguchi method has been utilized by many researchers to improve various machining operations in various alloys, such as turning, end milling, drilling, and so on [30]. The surface roughness of HSS steel was evaluated using Taguchi method. It was found that if servo voltage and servo feed are increased, the surface roughness value decreases, but increases as pulse duration and peak current are increased [31, 32]. The machining parameters varying the T_{on} , T_{off} , servo voltage, and peak current. The rate of material removal and the roughness of the surface were the performance parameters. Taguchi and ANOVA approaches were utilised to define the important factors [33]. Pramanik et al. [18] studied on Ti–6Al–4V and assessed for its performance. The titanium alloy was machined using the Wire EDM method. Process parameters included T_{on} , T_{off} , and wire tension. Ra, crack propagation, and fatigue life are taken into consideration. With a shorter T_{on} and a longer T_{off} , better results were obtained. L9 OA approach has been applied to optimise self-healing materials in research work [18–20]. Subrahmanyam et al. [20] had conducted experiment using wire EDM to study the effect of process parameters of Inconel 625 on MRR and Ra and also optimized using Taguchi method. From the experimental results it was found that pulse off time exhibited maximum contribution on MRR of 61.90% followed by T_{on} and peak current but for surface roughness, T_{on} has greatest impact of 67.09% followed by T_{off} and peak current. The optimal setting for MRR and Ra were A2B1C3 and A1B2C3. It was observed that with the chosen parameters the maximum

MRR and minimum Ra were obtained. Hareesh et al. [21] Evaluated the impact of wire EDM factors on the surface finish of Ti6Al4V. From the observations, the Ra increases with lower wire speed and a higher depth of cut. The better Ra was found at higher voltages. In between the voltage and wire speed, less interaction was observed from the interaction plot.

Goyal et al. [22] evaluated the wire breakage in wire EDM during machining of Nimonic 80A alloy. It was considered as the main factor affecting the Ra. From ANOVA, the factor that has the most impact on Ra is the duration of the pulse. The machining procedure in this investigation was performed using brass wire (Zinc coated). Tata et al. [23] performed the research work. The study aimed to determine how wire EDM affects INCONEL-625 machining. For roughness values (Ra) and material removal rate, grey relation analysis (GRA) is used to optimise these parameters. Both the MRR and Ra are affected by two parameters: T_{on} and T_{off} . Furthermore, it was identified that A2B1C3 is the best parameter setting for MRR. In addition, the best parameter setting for surface finish was found to be (A1B2C3).

The selection of suitable machining factors to achieve effectiveness and higher productivity under Wire EDM. The achievement of this optimization is crucial. From the available literature survey, the study on surface roughness and its optimization has been already carried out for various workpiece materials but for copper-based shape memory alloys no work has been carried out on machinability and its reports are not available till today because

it has been restricted to the synthesis of alloy only. The purpose of this study is to optimise the machinability factors to obtain an optimal value of Ra along with optimum surface finish, and to evaluate the effect of input factors on machinability of Cu–Al–Mn ternary SMAs using Wire EDM.

Experimental Work

Methodology

In this investigation, as a means of cutting, a 0.25 mm dia molybdenum wire is used to cut the cylindrical specimen (100xø12mm) of Cu–Al–Mn ternary SMAs. Figure 1 indicates the flow chart of the process. From Taguchi method, L9 orthogonal array was chosen to perform number of trails required to carry out the experiment. The SMAs are prepared using induction furnace and are machined using Wire EDM. The alloys which exhibited good shape memory effect were subject to machinability studies. At each cutting operation, the input process parameters were altered. The investigation was carried out to find the texture quality of the Cu–Al–Mn ternary SMA as input factors varies. The entire machining process utilized distilled water as dielectric medium. After the completion of nine trails, the surface roughness (SR) of Cu–Al–Mn ternary SMAs was measured using a digital surface roughness tester.

Fig. 1 Flow chart of the process



Table 1 Chemical composition of Cu–Al–Mn ternary SMAs

Alloy ID	Composition (wt.%)		
	Cu	Al	Mn
CAM1	88.5	10.5	1
CAM2	88	10	2
CAM3	86.5	10.5	3

**Fig. 2** As-cast samples of Cu–Al–Mn ternary SMAs

Chemical Composition of Cu–Al–Mn ternary SMAs

The chemical composition of the prepared Cu–Al–Mn ternary SMAs is listed in Table 1. Figure 2 indicates three as-cast samples of both cylindrical and flat samples. Flat sample is used to evaluate the SME and the cylindrical sample of that is subjected to study the machinability of the alloy under WEDM. The composition was determined using spark emission spectrometer.

Taguchi Design

The orthogonal array design proposed by Taguchi is an extremely helpful method for determining the major effects of a study with constrained experiments. These approaches allow for the investigation of primary effects even when the component being studied has more than two levels [10]. When analysing the variance, the Taguchi technique makes use of the S/N ratios. The reduction in the surface's roughness is the objective of this line of research. As a consequence of this, the S/N ratio for each of the L9 experiments was determined by employing the strategy "smaller is better." The outcome of this work was to measure the Ra value of machined samples determined using Mitutoyo surface roughness tester (SJ201).

Taguchi technique was utilized to design the experiment, and MINITAB 17 was used to find the best combination of factors to reach the desired goal of lowering the Ra and improving the quality of the cut. The purpose of the

Table 2 Process variables and its levels

Process variables	Level-1	Level-2	Level-3
Pulse duration (μ s)	100	105	110
Pulse interval (μ s)	25	28	32
Peak current (A)	1	2	3

Table 3 %SME of Cu–Al–Mn ternary SMAs

Sl. no	Alloy ID	%SME
1	CAM1	64.8
2	CAM2	75.24
3	CAM3	84.61

**Fig. 3** Hot-rolled samples of CAM1, CAM2 and CAM3 ternary SMAs

experiment was to accomplish the most accurate examination of the impacts of a variety of primary elements while at the same time minimising the amount of time spent doing the experiment by reducing the number of trials. The pulse duration, pulse interval, and peak current were the input factors and Ra as output response factor. The chosen factors are splitted into three levels, which are outlined in Table 2.

Results and Discussion

Shape Memory Effect (SME)

The property of the sample to regain its memory (shape) after deformations when subjected to heat or stresses. Table 3 gives the SME of 3 samples of Cu–Al–Mn ternary SMAs. The CAM3 ternary SMA exhibited maximum SME of 84.61%, hence the cylindrical specimen

of this composition was subjected to machinability studies in Wire EDM. Figure 3 shows the hot rolled samples of Cu–Al–Mn ternary SMAs which are used for further characterization.

Strain recovery by SME was calculated as

$$\%SME = \frac{\theta_m}{180 - \theta_e}$$

where θ_m = Recovery of the angle upon heating, θ_e = Recovery of the angle upon unloading (Spring back angle).

SEM Images of as Cast and Step Quenched Cu–Al–Mn SMAs

After the bend test the sheet specimens were cut to the required shape. The step-quenching process resulted in the formation of martensite structure as observed under SEM. The suitable cold setting agents were used to cold set the sheet sample. The cold set samples were polished in a polishing machine with various grids of emery papers (200, 400, 600, 800, 1000, 1200, and 2000) and finally, by using polishing cloth the sample was polished to obtain the mirror finish on the surface. The specimen was cleaned and dried with acetone. Keller's reagent (A few drops of etchant (100 ml water, 10 ml H₂SO₄, 4 drops Hydrochloric acid, 10 g potassium dichromate) were applied on the surface of both the as-cast and polished sheet specimens and allowed for 3–5 s and wipe off the etched surface with acetone. Finally, the as-cast and step quenched specimens were examined under the SEM. Figure 4 shows the parent austenite phase and Fig. 5 shows lath type martensite structure of CAM3 ternary SMA.

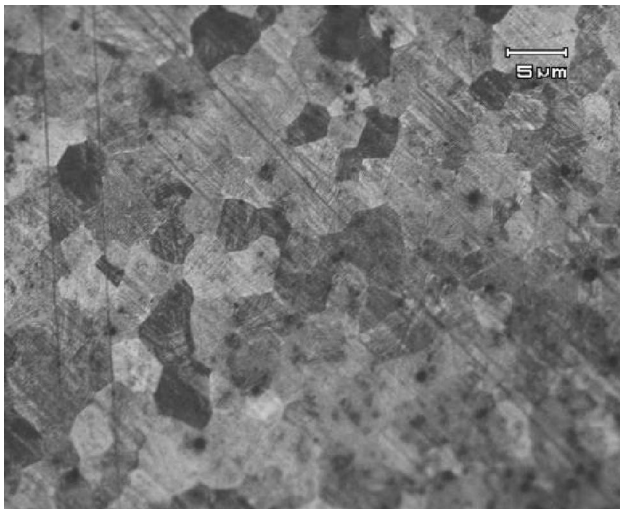


Fig. 4 Parent austenitic phase

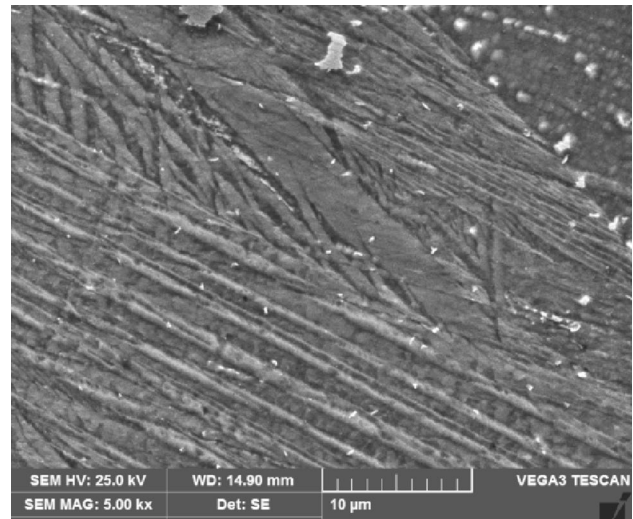


Fig. 5 Lath type martensite structure

Observations

The trials were planned based on Taguchi orthogonal array approach [24]. Orthogonal arrays are a type of fractional orthogonal design that features a high degree of fractionality [21]. In Table 4, Taguchi's L9 OA was selected and performed all the nine experiments with different sets of input parameters. After nine trials, the average surface roughness was measured on three surfaces using a Mitutoyo tester. Figure 6 indicates that the alloy which exhibited the maximum SME. Figure 7 shows the cylindrical specimen of CAM3 ternary SMA mounted in Wire EDM.

Surface Roughness (SR)

The machined samples were evaluated by assessing their surface roughness, and to examine the morphology formed in order to enhance the surface finish. The particles uniformly distributed results in uniform plastic deformation, there by reduces subsurface damage.

Analysis of Variance (ANOVA)

The S/N ratio is used to construct products and processes that are not affected by noise factors. This reveals the extent to which a product or process responds in a predictable manner despite the presence of noise factors. The data were analysed using the ANOVA, which aimed to find which factors had the most significant impact on the performance measure (Ra). The results of the ANOVA for both the mean and the standard deviation demonstrate that the pulse duration, the pulse interval, and the peak current are the three factors that have a significant impact on the SR. However, peak current is the factor that contributes the most to surface roughness.

Table 4 Machined data of Cu–Al–Mn SMAs under L9 OA

No. of trails	Pulse duration (μs)	Pulse interval (μs)	Peak current (A)	Surface Roughness (Avg. Ra)	S/N Ratio (db)
1	100	25	1	1.663	−4.418
2	100	28	2	2.058	−6.269
3	100	32	3	3.273	−10.3
4	105	25	2	2.775	−8.865
5	105	28	3	3.469	−10.8
6	105	32	1	1.5	−3.522
7	110	25	3	3.905	−11.83
8	110	28	1	1.827	−5.235
9	110	32	2	2.425	−7.694



Fig. 6 Cylindrical specimen of CAM3 ternary SMA

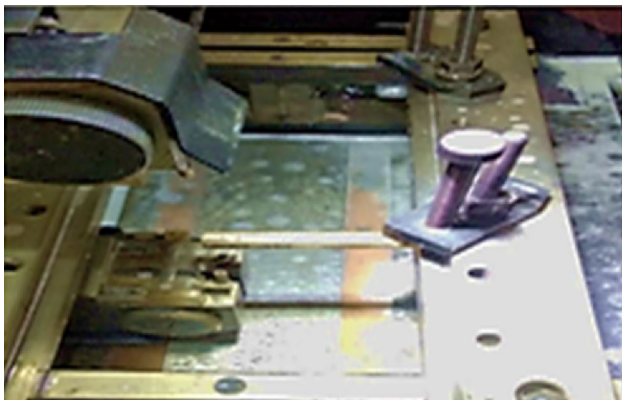


Fig. 7 Experimental setup of CAM3 ternary SMA in Wire EDM

Figure 8 depicts the main effect plot for the mean of SR, which shows how SR varies depending on the input parameters. This plot indicates how SR responds to changes in the parameters (Fig. 9).

Evaluation of S/N Ratio for Optimal Design

The S/N ratio is a statistical term that refers to the relationship between the mean and the standard deviation. The

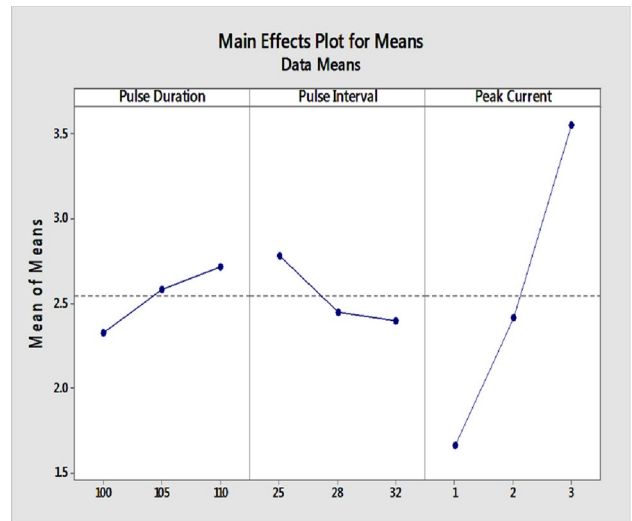


Fig. 8 Plot for means

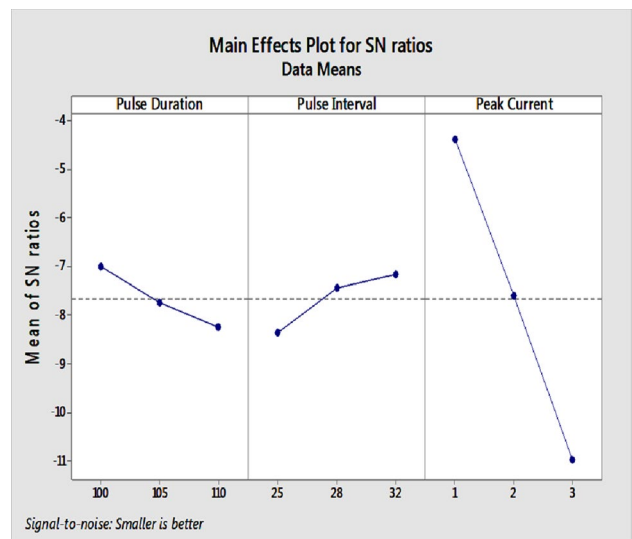


Fig. 9 Plot for S/N ratio

Table 5 Response table for S/N ratios

Smaller is better			
Levels	Pulse duration (A)	Pulse interval (B)	Peak current (C)
1	−6.995	−8.372	−4.391
2	−7.73	−7.436	−7.609
3	−8.254	−7.172	−10.978
Delta	1.259	1.2	6.587
Rank	2	3	1

Table 6 Response table for means

Levels	Pulse duration	Pulse interval	Peak current
1	2.331	2.781	1.663
2	2.581	2.451	2.419
3	2.719	2.399	3.549
Delta	0.388	0.982	1.889
Rank	2	3	1

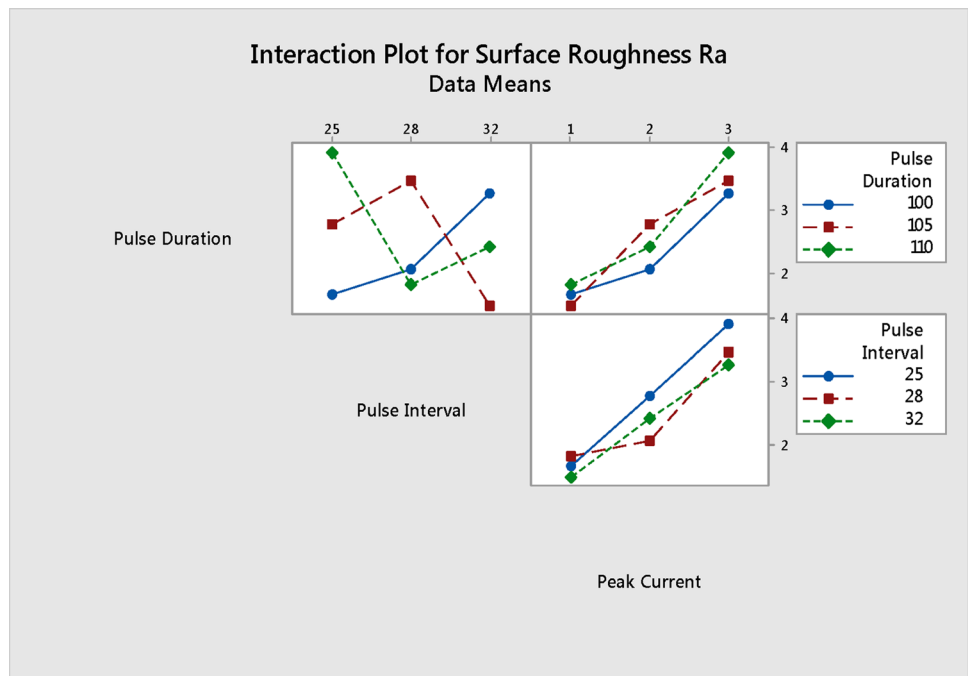
square of mean value of quality characteristics is represented by the signal, while the variability of characteristics is represented by noise. These S/N ratios are evaluated based on the response requirement. The analysis was designed using software MINITAB 17. “Smaller the better” approach was chosen to study the surface roughness of Cu–Al–Mn ternary SMA. From the observation, it was noticed that Ra rises with an increase in pulse duration and peak current. Tables 5 and 6 show S/N ratio and mean response table statistics. The optimum factor level in the experimental domain is the one

that indicates the highest S/N ratio value. The mean of each level of every factor are used to construct response table for SR which is given below.

From Tables 5 and 6, the results showed that the peak current is the most influential factor in determining the surface roughness, ranking first, followed by the pulse duration and the pulse interval. Figure 8 indicates the effect of input factors on Ra. According to the plot, the surface roughness increases along with an increase in pulse duration, and peak current while it reduces along with an increase in pulse interval. Because of the larger discharge energy and the greater intensity of the spark that exists between the wire and the SMA, this results in a greater amount of material being removed, which impacts an increase in the surface roughness value [19]. Because the time interval required removing the melted tiny particles from the gap between the tool and the SMA being machined is short, increasing the pulse interval reduces the surface roughness of Cu–Al–Mn ternary SMAs. In order to construct the major effect graphs, the average values of the parameters are taken into consideration for each level of the raw data. The plot showed the optimum level selected for SR is A1, B3, C1, i.e. pulse duration (100 μs), pulse interval (32 μs) and peak current (1A).

Figure 10 shows the interaction plot for surface roughness, which indicates the interaction of three different machining factors, like pulse duration, pulse interval, and peak current, on performance characteristics. An increase in the pulse duration does not showed any effect on the Ra when measured at a lower peak current of 1 A. From the plot, it was found that strong interactions exist between pulse duration, the pulse interval and peak current. Because the

Fig. 10 Interaction plot for SR



reactions obtained at various levels of process parameters are nearly identical [34–37].

Regression Analysis

It is a statistical way to find how a dependent variable and one or more independent variables are related. It can be used to find out how strong a relationship between two variables. The regression equation for surface roughness was obtained from MINITAB 17 software. From Table 7 it was noticed that the peak current has lesser probability (P) value which is lower than ($\alpha=0.05$), which shows the present model is significant. The percentage contribution for peak current is (90.04%) compared to other factors such as pulse duration (3.81%) and pulse interval (3.41%). Hence, peak current has to be controlled to obtain better surface finish with a minimum surface roughness. From Table 8 indicates regression coefficients, P value is lower than ($\alpha=0.05$). The F -ratios indicate whether a selected factors are important or not at a given confidence level. If the F -ratio is high, then it is more likely that even a little change in the value of one of the process parameters will have a significant effect on the output response. The regression square value obtained is (97.26%) and the regression square adjacent (97.62%). The predicted regression square obtained is (90.91%). Equation 1 is the representation of the regression equation that was computed for the surface roughness.

$$Ra = -1.93 + 0.0388 \text{ Pulse duration} - 0.0523 \text{ Pulse interval} + 0.9428 \text{ Peak current} \quad (1)$$

Confirmation Test

The confirmation test performed in accordance with the optimal level that the analysis of means had suggested. Experiments were carried out so that the optimization of the L9 Orthogonal array could be verified. Table 8 displays the average experimental readings and the theoretical values for surface roughness. As a result of all three trials, it has been demonstrated that the variation in inaccuracy between the experimental data and the theoretical values for surface roughness is less than 5%. It illustrates that the results are

Table 8 Confirmation test

No. of trails	Experimental value	Theoretical value	% Error
1	2.1596	2.1556	0.181
2	3.1277	3.1237	0.125
3	3.3835	3.3796	0.116

very reproducible and that the optimised process parameters and response values match experimental values. Furthermore, it illustrates that the results may be reproduced to achieve greater accuracy. As a result of using the best possible settings for the input parameters, the value of the Ra was calculated to be ($Ra = 1.2192 \text{ m}$). The measured surface roughness falls somewhere in the range covered by the confidence levels.

SEM Analysis of Machined Sample of Cu–Al–Mn Ternary SMAs

The Wire EDM technique generates a sequence of sparks that help to melt the material off the work area [38]. In the WEDM process, to produce good surface quality free of micro-cracks, micro-pores, and other surface defects, the process parameters must be controlled. Greater values of T_{on} and current result in a larger discharge energy. This is because of an increase in the intensity of the spark which enhances to the formation of micro-cracks, globules, micro-pores, and other surface flaws to occur [39, 40]. A longer pulse-off time, on the other hand, reduces the discharge energy level and, as a result, the creation of micro-cracks, globules, micro-pores, and other surface defects. At both low and high discharge energies, the morphology formed was analysed in detail.

Figures 11 and 12 show SEM micrographs of the machined surface taken at low (pulse duration-100 μs , pulse interval-25 μs and peak current-1A) and high (pulse duration-110 μs , pulse interval-32 μs and peak current-3A) discharge energy levels. When compared to the low discharge energy level, it was made abundantly clear that, at the high discharge energy level, micro-cracks, micro-pores, and deposited layers formed more readily, and globule diameters increased.

Table 7 ANOVA for surface roughness

Source	DF	Adj-SS	Adj-MS	F -value	P -value	% contribution
Pulse duration	1	0.2254	0.22543	6.96	0.046	3.81%
Pulse interval	1	0.2023	0.20225	6.24	0.055	3.41%
Peak current	1	5.3336	5.33361	164.61	0.000	90.04%
Error	5	0.162	0.324			2.74%
Total	8	5.9233				100%

$S = 0.180002$; $R\text{-sq} = 97.26\%$; $R\text{-sq (adj)} = 97.62\%$; $R\text{-sq (Pred)} = 90.91\%$

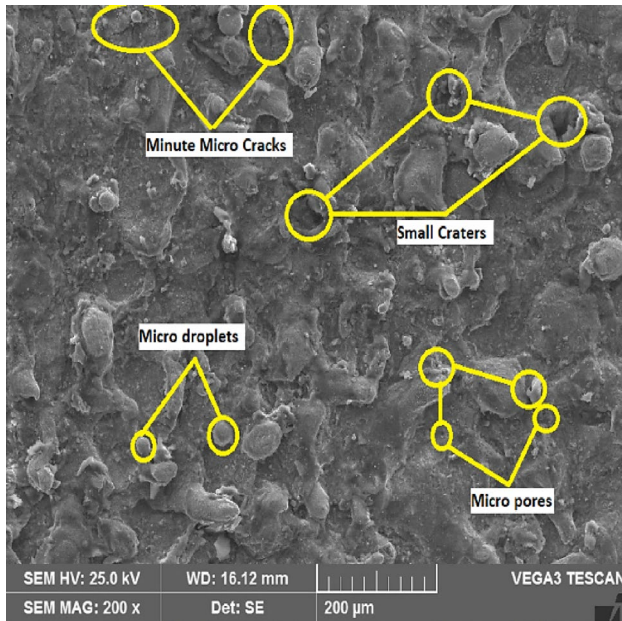


Fig. 11 Image of surface machined at low discharge energy level

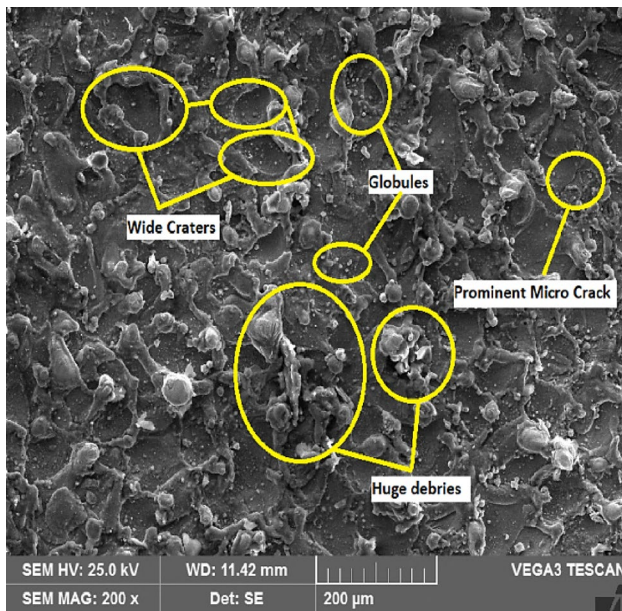


Fig. 12 Image of surface machined at high discharge energy level

This was demonstrated in a clear and convincing manner. At the high discharge energy level, the material easily melts and evaporates, which then combines with the dielectric fluid [41–44]. The material is cooled in the dielectric fluid after it has been brought into contact with it. This quenching event causes cracks, porosity, and other flaws to emerge [45–48]. Furthermore, high discharge energy accelerates material removal. As a consequence of the elimination of superfluous

material, certain debris particles are left out on the surface that has been machined.

The phenomena of quenching and material deposition are greatly minimised compared to high discharge energy. As a direct consequence of this, Fig. 11 demonstrates a limited amount of micro-cracks, micro-pores, deposited layers, and microscopic debris. However, it is extremely difficult to completely eradicate micro-pores, micro-cracks, debris, and deposited layers because the WEDM process will always have some level of discharge energy present, regardless of the parameter settings that are chosen. Figures 11 and 12 show that at low discharge energy, the crater size is minimised and less material is removed. But the size and number of debris, craters and micro-pores increases at higher discharge energy [49–53].

This phenomena show that reduced discharge energy improves surface integrity. WEDM characteristics at the lowest discharge energy, on the other hand, it is not possible to reach the overall objectives. In order to achieve a greater MRR, T_{on} , and current, it is required to use a higher discharge energy along with maintaining a lower T_{off} level. Using a lower energy level for the discharge while maintaining a higher T_{off} is required in order to achieve a lower SR, lower T_{on} , and lower current. Adjusting the settings of the WEDM to achieve optimal performance in order to accommodate multiple responses is an effective method for addressing this conflicting situation. For the WEDM process to successfully machine Cu–Al–Mn SMA, the discharge current, T_{on} , and T_{off} parameters must be set to their optimal values. A machined surface with optimal parameter settings is shown in Fig. 13a. In this situation, the existence of micro-cracks, micro-pores, and micro-droplets is optimal in comparison to the greater discharge energy level. Figure 13a shows that the work surface is free of Mo.

Figure 13b shows EDAX results of wire EDM-machined surface. The image was taken from the centre of the sample. The values of the chemical components that were reported were produced using the EDX analysis that was performed on the SEM, which provides accurate values. It has been found through research conducted in the past that using brass wire as tool will result in deposition on the surface that has been machined [32, 33]. The present study utilized the reusable molybdenum wire as tool material for machining Cu–Al–Mn SMA. All additional elements like O, Cu, Al, and Mn are taken into account during an EDAX evaluation of a machined surface. The EDX examination revealed low oxygen content and high Cu, Al and Mn concentrations.

Because of the selection of these characteristics, it was feasible to machine the alloy without leaving any deposits. Molybdenum has a very high melting point, and it has a low propensity for chemical reactions [54, 55]. As a consequence of this, there are less opportunities for there to be a material dispute between the workpiece and the molybdenum wire

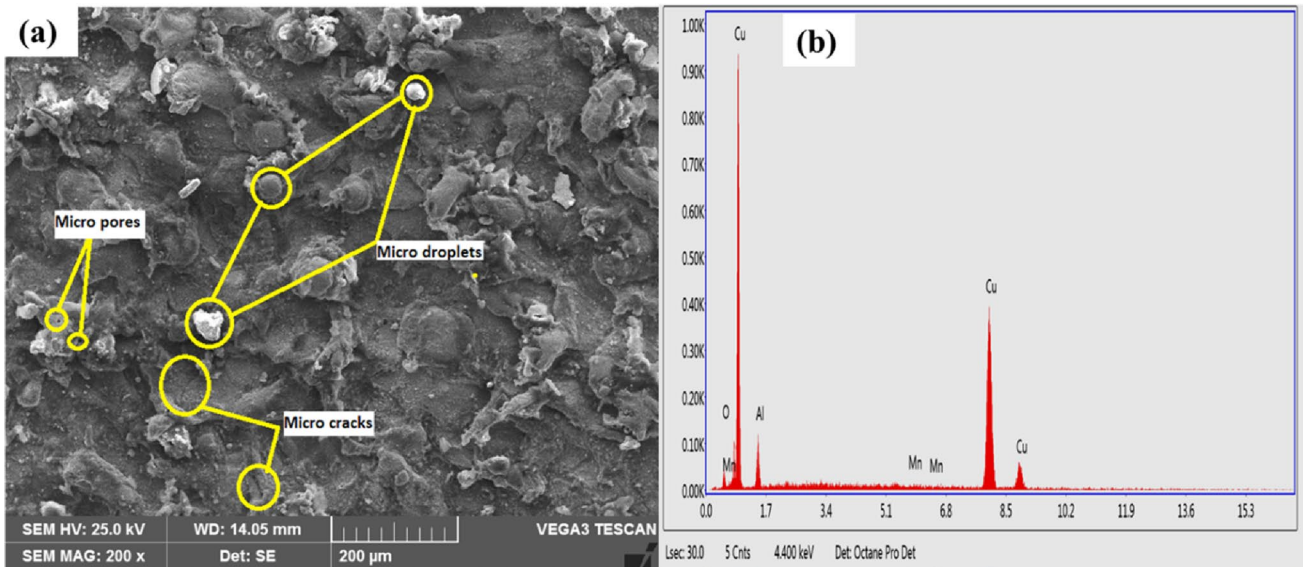


Fig. 13 a Machined surface of Cu–Al–Mn SMAs at optimum setting (A1B3C1), b EDAX study using optimum process conditions

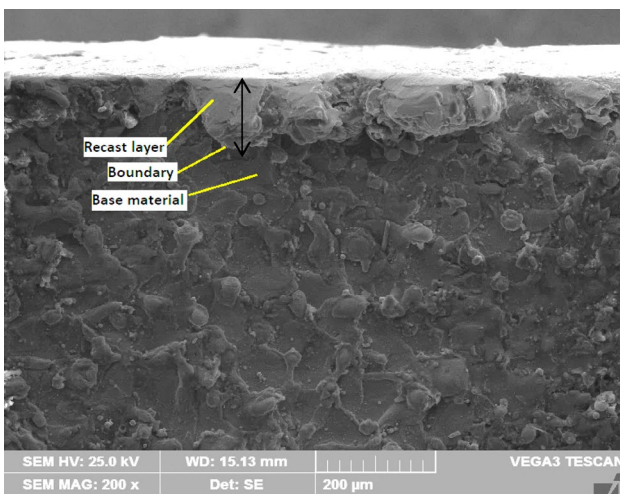


Fig. 14 C/S view of Cu–Al–Mn SMAs at optimum setting condition (A1B3C1)

[45–48]. Because of this, the material from the wire did not get deposited on the working surface. Wire EDM shows how effectively the tool electrode works with Cu–Al–Mn SMA. Figure 14 indicates the cross-sectional view of the machined sample for an optimum condition (A1B3C1). It was seen that there was a layer on the surface, and it was adjacent to the boundary. These surface layers are whitish in colour (also called the "recast layer."). Due to the presence of oxides, the white layer is usually harder than the rest of the material [56–60]. The presence of a recast layer in Wire EDM machined Cu–Al–Mn shape memory alloys can have implications for the surface quality, dimensional accuracy, and mechanical properties of the machined part.

The recast layer may have different microstructural characteristics compared to the base material, such as altered grain structure or composition, which can affect the functional properties of the shape memory alloy. To minimize the formation of a recast layer and mitigate its potential negative effects, process optimization techniques can be employed. These include adjusting the machining parameters, such as pulse duration, energy settings, and flushing conditions, to optimize the material removal rate while minimizing the recast layer thickness and preserving the desired properties of the shape memory alloy.

Discussion

WEDM offer several advantages when it comes to machining Cu–Al–Mn shape memory alloys (SMAs). Here are some justifications for the advantages of CNC WEDM in the present application:

CNC WEDM utilizes advanced computer controls and programming to execute precise and accurate machining operations. This is particularly important when working with Cu–Al–Mn SMAs, as their shape memory properties and intricate designs often require high precision. CNC control ensures consistent and repeatable cutting, resulting in components with tight tolerances and excellent dimensional accuracy. Cu–Al–Mn SMAs often require intricate and complex shapes due to their unique applications. CNC wire EDM excels at machining complex shapes and contours with ease. The wire can be programmed to follow intricate paths, allowing for the production of intricate and intricate components that may be challenging to achieve with other

machining methods. Cu–Al–Mn SMAs are sensitive to heat and mechanical stress, which can affect their shape memory properties. CNC WEDM operates at a relatively low temperature compared to traditional machining methods like milling or turning. This low-heat machining reduces the risk of thermal distortion or undesirable phase transformations in the material, preserving the shape memory properties of the alloy. The addition of Cu content on Cu-based SMA increases martensitic temperature [37]. CNC WEDM can achieve exceptional surface finishes, even on difficult-to-machine materials like Cu–Al–Mn SMAs. The controlled electrical discharge process used in wire EDM erodes the material, resulting in a smooth surface texture. This is particularly advantageous in applications where a high-quality surface finish is necessary, such as medical devices or aerospace components. CNC WEDM machines are highly automated, allowing for unmanned or lights-out operation. Once the programming is set, the machine can run continuously, reducing operator intervention and increasing productivity. This level of automation is beneficial in industries where high-volume production or extended machining times are required. CNC wire EDM machines are versatile and can be used to machine a wide range of shapes, sizes, and thicknesses of Cu–Al–Mn SMAs. The programming flexibility enables the production of custom components and the ability to adapt to changing design requirements. These advantages contribute to the production of high-quality components with tight tolerances, preserving the unique properties of shape memory alloys.

Cu–Al–Mn shape memory alloys (SMAs) have some drawbacks associated with their machining using Wire EDM. Here are a few limitations supported by the literature: Cu–Al–Mn SMAs have poor machinability compared to conventional materials like steels or aluminium alloys. The presence of shape memory effects and the alloy's unique microstructure, including the formation of ordered phases, can make machining more challenging. According to a study by Zhang et al. (2018) titled "Machinability investigation of copper-based shape memory alloys," the machinability of Cu–Al–Mn SMAs is lower than that of other copper-based alloys due to their higher strength and lower thermal conductivity. During Wire EDM machining, the localized heat generated can induce work hardening in the machined surface of Cu–Al–Mn SMAs. Work hardening can result in increased hardness and reduced ductility, potentially affecting the shape memory properties of the alloy. "Electrical discharge machining of shape memory alloys: A review" highlights the issue of work hardening during EDM machining and its impact on the surface integrity of shape memory alloys. Wire EDM can induce residual stresses in the machined surface of Cu–Al–Mn SMAs. These residual stresses may affect the shape memory behaviour and mechanical properties of the alloy. Additionally, Wire EDM

can lead to relatively higher surface roughness compared to other machining methods [12–14]. "Experimental study on surface integrity of Cu–Al–Mn shape memory alloy in wire electrical discharge machining" discusses the formation of surface cracks, micro-craters, and roughness in Cu–Al–Mn SMA specimens after Wire EDM [25, 30].

Wire EDM is known for its slower material removal rate compared to some other machining methods. The process involves the erosion of material through controlled electrical discharges, which can limit the efficiency and productivity when machining Cu–Al–Mn SMAs. The relatively low material removal rate in copper-based shape memory alloys. It is important to consider these drawbacks and limitations when utilizing wire EDM for machining Cu–Al–Mn shape memory alloys. Proper process optimization, selection of machining parameters, and understanding the material behaviour can help mitigate these challenges and ensure the desired quality and functionality of the machined components [1–8].

Conclusions

The following are the conclusion drawn from the present investigation.

- The Cu–Al–Mn ternary SMAs were synthesized and characterized to check for its machinability with reference to resulting surface roughness obtained under Wire EDM. From the bend test, the maximum SME of 84.61% was obtained for CAM3 SMA as compared to CAM1 and CAM2 SMAs.
- From ANOVA it was found that the peak current has the greatest significance on Ra, whereas the other two parameters (pulse duration and pulse interval) had a lesser impact on Ra. The value of Ra has been optimised, and the results of the optimization have been confirmed by means of a confirmation trial. The difference between the theoretical and experimental values of SR is less than 5%, according to the error analysis that was performed.
- From Taguchi Analysis, the optimal machining variables of combination setting are, pulse duration (100) μ s, pulse interval (32) μ s and peak current (1) A to obtain the optimum Ra. Also, the peak current should be kept to a minimum to achieve a better surface finish. During machining of Cu–Al–Mn SMA, a significant amount of uncleaned debris and micro-pores were present, which were clearly visible through SEM morphology analysis at higher discharge energy levels. Maximum MRR is produced by the obvious crack forms and massive debris. The optimum parameter settings reduced micro-cracks, micro-pores, and craters compared to a high discharge energy level.

- Wire EDM machining of Cu–Al–Mn shape memory alloys, including good surface texture, precision, minimal material stress, and the ability to create complex shapes. These characteristics make it a valuable method for manufacturing high-quality components and devices using shape memory alloys in industries that require superior surface finishes and intricate designs.

Acknowledgements The authors would like to take this opportunity to extend their appreciation to the Siddaganga Institute of Technology for the research assistantship support that was provided in order to carry out this research work.

Funding The authors have not disclosed any funding.

Declarations

Conflict of interest The authors declare that they have no conflict of interest.

References

1. S. Balasubramani, T. Vigraman, Effect of Cu and Ti addition in Fe–Mn–Si shape memory alloy. *Int. J. Sci. Eng. Res.* **5**(5), 183–186 (2014)
2. I. Journal, O.F. Engineering, A.R. On, O. Detection, a review on obstacle detection and vision. *Int. J. Eng. Sci. Res. Technol.* **4**(1), 1–11 (2015)
3. U.S. Mallik, V. Sampath, Influence of quaternary alloying additions on transformation temperatures and shape memory properties of Cu–Al–Mn shape memory alloy. *J. Alloys Compd* **469**, 156–163 (2009)
4. U.S. Mallik, V. Sampath, Influence of aluminum and manganese concentration on the shape memory characteristics of Cu–Al–Mn shape memory alloys. *J. Alloys Compd.* **459**(1–2), 142–147 (2008)
5. U.S. Mallik, V. Sampath, Effect of composition and ageing on damping characteristics of Cu–Al–Mn shape memory alloys. *Mater. Sci. Eng. A* **478**, 48–55 (2008)
6. D. Gajjar, J. Desai, Optimization of MRR, surface roughness and KERF width in wire EDM using Molybdenum wire. *Int. J. Res. Educ.* **4**(2), 9–17 (2015)
7. P.V.D. Patel, R.V. Vaghmare, A Review of recent work in wire electrical discharge machining. *IJERA* **3**(3), 805–816 (2013)
8. F. Kausar, S. Kumar, M. Azam, S. Suman, A. Sharma, A. Sethi, Optimization of machining parameter for surface roughness on Wedm of En36 alloy steel. *IOSR J. Mech. Civ. Eng. Ver. II* **12**(6), 2278–2684 (2015)
9. P. Bharathi, T. Gouri, L. Priyanka, G.S. Rao, B.N. Rao, Optimum WEDM process parameters of SS304 using taguchi method. *Int. J. Ind. Manuf. Syst. Eng.* **1**(3), 69–72 (2016)
10. M.D. Prakash, R.S. Narayanan, Prediction of machining parameters on tool steel in wire EDM. *Int. J. Innov. Res. Sci. Eng. Technol.* **27**, 10618–10624 (2016)
11. G. Archana, K. Dharma Reddy, P. Venkataramaiah, Study on machining response in wire EDM OF Inconel 625. *Int. J. Appl. Eng. Res.* **13**(21), 15270–15277 (2018)
12. M.S. Hewidy, T.A. El-Taweel, M.F. El-Safty, Modelling the machining parameters of wire electrical discharge machining of Inconel 601 using RSM. *J. Mater. Process. Technol.* **169**, 328–336 (2005)
13. B. Hwa Yan, H.C. Tsai, F. Yuan Huang, L. Chong Lee, Examination of wire electrical discharge machining of Al₂O₃p/6061Al composites. *Int. J. Mach. Tools Manuf.* **45**(3), 251–259 (2005)
14. P.N. Singh, K. Raghukandan, B.C. Pai, Optimization by Grey relational analysis of EDM parameters on machining Al-10%SiC P composites. *J. Mater. Process. Technol.* **155–156**(1–3), 1658–1661 (2004)
15. M.H. El-Axir, M.M. Elkhabeery, M.M. Okasha, Modeling and parameter optimization for surface roughness and residual stress in dry turning process. *Eng. Technol. Appl. Sci. Res.* **7**(5), 2047–2055 (2017)
16. S. Hammed, V.N. Najm, Surface Roughness Evaluation in WEDM Using Taguchi Parameter Design Method. *Eng. Technol. J.* **36**(1), 10–1102 (2018). <https://doi.org/10.30684/etj.36.1A.9>
17. H.T.T. Alloy, Revealing the WEDM process parameters for the machining of. pp. 1–15 (2021)
18. A. Pramanik, A.K. Basak, Effect of wire electric discharge machining (EDM) parameters on fatigue life of Ti–6Al–4V alloy. *Int. J. Fatigue* **128**, 105186 (2019)
19. M. Manjaiah, S. Narendranath, J. Akbari, Optimization of wire electro discharge machining parameters to achieve better MRR and surface finish. *Procedia Mater. Sci.* **5**, 2635–2644 (2014)
20. M. Subrahmanyam, T. Nancharaiah, Optimization of process parameters in wire-cut EDM of Inconel 625 using Taguchi's approach. *Mater. Today Proc.* **23**, 642–646 (2020)
21. K. Hareesh, K.V. Nalina Pramod, N.K. Linu Husain, K.B. Binoy, R. Dipin Kumar, N.K. Sreejith, Influence of process parameters of wire EDM on surface finish of Ti6Al4V. *Mater. Today Proc.* **47**, 5017–5023 (2021)
22. A. Goyal, A. Garimella, P. Saini, Optimization of surface roughness by design of experiment techniques during wire EDM machining. *Mater. Today Proc.* **47**, 3195–3197 (2021)
23. N. Tata, R.K. Pacharu, S.K. Devarakonda, Multi response optimization of process parameters in wire-cut EDM on INCONEL 625. *Mater. Today Proc.* **47**, 6960–6964 (2021)
24. S. Paliwal, P. Solanki, M. Soni, A.K. Chanda, Parameter optimization of wire electrical discharge machining for minimum surface roughness and Kerf width using Taguchi method. *Int. J. Ind. Electron. Electr. Eng.* **2**(7), 36–39 (2014)
25. A. Goyal, A. Pandey, P. Sharma, Investigation of surface roughness for Inconel 625 using wire electric discharge machining. *IOP Conf. Ser. Mater. Sci. Eng.* **377**, 1 (2018)
26. A.M. Takale, N.K. Chougule, R.L. Patil, A.S. Awate, Analysis and optimization of wire electro discharge machining parameters of TiNi shape memory alloy using Taguchi technique. *SSRN Electron. J.* (2018). <https://doi.org/10.2139/ssrn.3101586>
27. C.J. Manjunatha, C. Durga Prasad, H. Hanumanthappa, A. Rajesh Kannan, D.G. Mohan, B.K. Shanmugam, C. Venkatesgowda, Influence of microstructural characteristics on wear and corrosion behaviour of Si₃N₄ reinforced Al2219 composites. *Adv. Mater. Sci. Eng. Hindawi*, vol. 2023, Article ID 1120569, (2023) <https://doi.org/10.1155/2023/1120569>
28. H. Sharanabasva, C. Durga Prasad, M.R. Ramesh, Characterization and wear behavior of NiCrMoSi microwave cladding. *J. Mater. Eng. Perform.* (2023). <https://doi.org/10.1007/s11665-023-07998-z>
29. H. Sharanabasva, C. Durga Prasad, M.R. Ramesh, Effect of Mo and SiC reinforced NiCr microwave cladding on microstructure, mechanical and wear properties. *J. Inst. Eng. (India) Series D* (2023). <https://doi.org/10.1007/s40033-022-00445-8>
30. K.H. Ho, S.T.Á. Newman, S. Rahimifard, R.D. Allen, State of the art in wire electrical discharge machining (WEDM). *Int. J. Mach. Tools Manuf.* **44**, 1247–1259 (2004)

31. F. Ghanem, C. Braham, H. Sidhom, Influence of steel type on electrical discharge machined surface integrity. *J. Mater. Process. Technol.* **142**, 163–173 (2003)
32. H.S. Nithin, K.M. Nishchitha, D.G. Pradeep, C. Durga Prasad, M. Mathapati, Comparative analysis of CoCrAlY coatings at high temperature oxidation behavior using different reinforcement composition profiles. *Weld. World* **67**, 585–592 (2023). <https://doi.org/10.1007/s40194-022-01405-2>
33. D.C. Naveen, N. Kakur, B.S. Keerthi Gowda, G. Madhu Sudana Reddy, C. Durga Prasad, R. Shanmugam, Effects of polypropylene waste addition as coarse aggregate in concrete: experimental characterization and statistical analysis. *Adv. Mater. Sci. Eng. Hindawi*, vol. 2022, Article ID 7886722, 11 pages (2022) <https://doi.org/10.1155/2022/7886722>.
34. V. Gowda, H. Hanumanthappa, B. Kumar Shanmugam, C. Durga Prasad, T.N. Sreenivasa, M.S. Rajendra Kumar, High-temperature tribological studies on hot forged Al6061-TiB₂ in-situ composites. *J. Bio Tribo-Corros.* **8**, 101 (2022). <https://doi.org/10.1007/s40735-022-00699-5>
35. G. Madhusudana Reddy, C. Durga Prasad, P. Patil, N. Kakur, M.R. Ramesh, Elevated temperature erosion performance of plasma sprayed NiCrAlY/TiO₂ coating on MDN 420 steel substrate. *Surf. Topogr.: Metrol. Prop.* **10**, 025010 (2022). <https://doi.org/10.1088/2051-672X/ac6a6e>
36. K.K. Jangra, An experimental study for multi-pass cutting operation in wire electrical discharge machining of WC-5.3% Co composite. *Int. J. Adv. Manuf. Technol.* **76**(5), 971–982 (2015)
37. R. Magabe, N. Sharma, K. Gupta, J.P. Davim. Modeling and optimization of Wire-EDM parameters for machining of Ni 55.8 Ti shape memory alloy using hybrid approach of Taguchi and NSGA-II. pp. 1703–1717 (2019)
38. G. Madhusudana Reddy, C. Durga Prasad, G. Shetty, M.R. Ramesh, T. Nageswara Rao, P. Patil, Investigation of thermally sprayed NiCrAlY/TiO₂ and NiCrAlY/Cr₂O₃/YSZ cermet composite coatings on titanium alloys. *Eng. Res. Express* **4**, 025049 (2022). <https://doi.org/10.1088/2631-8695/ac7946>
39. G. Madhusudana Reddy, C. Durga Prasad, G. Shetty, M.R. Ramesh, T. Nageswara Rao, P. Patil, High temperature oxidation behavior of plasma sprayed NiCrAlY/TiO₂ & NiCrAlY /Cr₂O₃/YSZ coatings on titanium alloy. *Weld World* **66**, 1069–1079 (2022). <https://doi.org/10.1007/s40194-022-01268-7>
40. T. Naik, M. Mathapathi, C. Durga Prasad, H.S. Nithin, M.R. Ramesh, Effect of laser post treatment on microstructural and sliding wear behavior of HVOF sprayed NiCrC and NiCrSi coatings. *Surf. Rev. Lett.* **29**(1), 225000 (2022). <https://doi.org/10.1142/S0218625X2250007X>
41. G. Madhusudana Reddy, C. Durga Prasad, G. Shetty, M.R. Ramesh, T. Nageswara Rao, P. Patil, High temperature oxidation studies of plasma sprayed NiCrAlY/TiO₂ & NiCrAlY /Cr₂O₃/YSZ cermet composite coatings on MDN-420 special steel alloy. *Metall. Microstruct. Anal.* **10**, 642–651 (2021). <https://doi.org/10.1007/s13632-021-00784-0>
42. M. Mathapati, C. Kiran Amate, C. Durga Prasad, M.L. Jayavardhana, T. Hemanth Raju, A review on fly ash utilization. *Mater. Today Proc.* **50**(Part 5), 1535–1540 (2022)
43. R. Dinesh, S. Rohan Raykar, T.L. Rakesh, M.G. Prajwal, M. Shashank Lingappa, C. Durga Prasad, Feasibility study on MoCoCrSi/WC-Co cladding developed on austenitic stainless steel using microwave hybrid heating. *J. Mines Metals Fuels* **69**(12A), 260 (2021). <https://doi.org/10.18311/jmmf/2021/30113>
44. N. Sharma, K. Gupta, J. Paulo, ScienceDirect on wire spark erosion machining induced surface integrity of Ni 55.8 Ti shape memory alloys. *Arch. Civ. Mech. Eng.* **19**(3), 680–693 (2019)
45. H. Bisaria, P. Shandilya, The machining characteristics and surface integrity of Ni-rich NiTi shape memory alloy using wire electric discharge machining. *J. Mech. Eng. Sci.* **233**(3), 1068–1078 (2019). <https://doi.org/10.1177/0954406218763447>
46. M. Azam, M. Jahanzaib, J.A. Abbasi, M. Abbas, A. Wasim, S. Hussain, Parametric analysis of recast layer formation in wire-cut EDM of HSLA steel. *Int. J. Adv. Manuf. Technol.* **87**, 713–722 (2016)
47. M. Sudana Reddy, C. Durga Prasad, P. Patil, M.R. Ramesh, N. Rao, Hot corrosion behavior of plasma sprayed NiCrAlY/TiO₂ and NiCrAlY/Cr₂O₃/YSZ cermets coatings on alloy steel. *Surf. Interfaces* **22**, 100810 (2021). <https://doi.org/10.1016/j.surfin.2020.100810>
48. C. Durga Prasad, M.R. Sharnappa Joladarashi, M.S. Ramesh, S. Srinath, Microstructure and tribological resistance of flame sprayed CoMoCrSi/WC-CrC-Ni and CoMoCrSi/WC-12Co composite coatings Remelted by microwave hybrid heating. *J. Bio Tribo-Corros.* **6**, 124 (2020). <https://doi.org/10.1007/s40735-020-00421-3>
49. T.R. Newton, S.N. Melkote, T.R. Watkins, R.M. Trejo, L. Reister, Investigation of the effect of process parameters on the formation and characteristics of recast layer in wire-EDM of Inconel 718. *Mater. Sci. Eng. A* **513–514**(C), 208–215 (2009)
50. V. Lalwani, P. Sharma, C.I. Pruncu, D.R. Unune. Response surface methodology and artificial neural network-based models for predicting performance of wire electrical discharge machining of inconel 718 alloy. *J. Manufact. Mater. Process.* **4**(2), 44 (2020). <https://doi.org/10.3390/jmmp4020044>
51. C. Durga Prasad, A. Jerri, M.R. Ramesh, Characterization and sliding wear behavior of iron based metallic coating deposited by HVOF process on low carbon steel substrate. *J. Bio and Tribo-Corros.* (2020). <https://doi.org/10.1007/s40735-020-00366-7>
52. C. Durga Prasad, S. Joladarashi, M.R. Ramesh, M.S. Srinath, B.H. Channabasappa, Comparison of high temperature wear behavior of microwave assisted HVOF sprayed CoMoCrSi-WC-CrC-Ni/WC-12Co composite coatings. *SILICON* **12**, 3027–3045 (2020). <https://doi.org/10.1007/s12633-020-00398-1>
53. C. Durga Prasad, S. Joladarashi, M.R. Ramesh, M.S. Srinath, B.H. Channabasappa, Effect of microwave heating on microstructure and elevated temperature adhesive wear behavior of HVOF deposited CoMoCrSi-Cr₃C₂ composite coating. *Surf. Coat. Technol.* **374**, 291–304 (2019)
54. C. Durga Prasad, S. Joladarashi, M.R. Ramesh, M.S. Srinath, B.H. Channabasappa, Development and sliding wear behavior of Co-Mo-Cr-Si cladding through microwave heating. *SILICON* **11**, 2975–2986 (2019). <https://doi.org/10.1016/j.surfcoat.2019.05.056>
55. C. Durga Prasad, S. Joladarashi, M.R. Ramesh, M.S. Srinath, B.H. Channabasappa, Microstructure and tribological behavior of flame sprayed and microwave fused CoMoCrSi/CoMoCrSi-Cr₃C₂ coatings. *Mater. Res. Express* **6**, 026512 (2019). <https://doi.org/10.1088/2053-1591/aaebd9>
56. C. Durga Prasad, S. Joladarashi, M.R. Ramesh, M.S. Srinath, B.H. Channabasappa, Influence of microwave hybrid heating on the sliding wear behaviour of HVOF Sprayed CoMoCrSi Coating. *Mater. Res. Express* **5**, 086519 (2018). <https://doi.org/10.1088/2053-1591/aad44e>
57. C. Durga Prasad, S. Joladarashi, M.R. Ramesh, A. Sarkar, High temperature gradient cobalt based clad developed using microwave hybrid heating. *Am. Inst. Phys.* **1943**, 020111 (2018). <https://doi.org/10.1063/1.5029687>
58. K.G. Girisha, C. Durga Prasad, K.C. Anil, K.V. Sreenivas Rao, Dry sliding wear behaviour of Al₂O₃ coatings for AISI 410 grade stainless steel. *Appl. Mech. Mater.* **766–767**, 585–589 (2015). <https://doi.org/10.4028/www.scientific.net/AMM.766-767.585>
59. K.G. Girisha, R. Rakesh, C. Durga Prasad, K.V. Sreenivas Rao, Development of corrosion resistance coating for AISI 410 grade steel. *Appl. Mech. Mater.* **813–814**, 135–139 (2015). <https://doi.org/10.4028/www.scientific.net/AMM.813-814.135>

60. R.R. Kolhapure, *Study of Machining Characteristics of Non-Conventional Methods*, vol. 2 (Atlantis Press International, Amsterdam, 2023)

Publisher's Note Springer Nature remains neutral with regard to jurisdictional claims in published maps and institutional affiliations.

Springer Nature or its licensor (e.g. a society or other partner) holds exclusive rights to this article under a publishing agreement with the author(s) or other rightsholder(s); author self-archiving of the accepted manuscript version of this article is solely governed by the terms of such publishing agreement and applicable law.